# Fabrication Errors Influence on the Spherical Array Radiation Pattern

*Slavko RUPCIC, Vanja MANDRIC , Snjezana RIMAC-DRLJE*

Laboratory for HF Measurements, J.J.Strossmayer University of Osijek, Kneza Trpimira 2b, 31000 Osijek, Croatia

rupcic@etfos.hr, vanja.mandric@etfos.hr, snjezana.rimac@etfos.hr

***Abstract.*** *The paper studies fabrication errors influence on the radiation pattern of a spherical antennas array. The developed Moment Method (MoM) program analyzes a particular influence of an azimuth and elevation position and local angle errors of antenna elements as well as model dimension errors on the radiation pattern. The spectral domain approach to the analysis of the spherical antenna arrays is applied here. Finally, results obtained from the theoretical investigation are verified by comparison with measured results.*

## Keywords

Radiation pattern, antenna array, aperture antenna, spherical array, fabrication errors, experimental model errors

## 1. Introduction

New generations of wireless communication systems, such as broadband wireless access networks and four generation (4G) mobile systems should provide different broadband services by using high data rates. Usage of the increasing bandwidths on higher frequencies, as well as smart antenna arrays can provide an efficient way to increase the data rate in future wireless systems. Smart antennas combine the antenna array with signal processing to optimize automatically the beam-pattern in response to the received signal. Array antennas can be designed to offer fast electronic beam-steering capabilities, reconfigurability, conformal characteristics, multi-beam capabilities and adaptive pattern reshaping. Some of the applications where these characteristics are desired also require that one or more beams can be steered in a wide angle in both azimuth and elevation. It is hard to achieve that with planar array antennas, because they suffer from pattern deterioration as the desired scan angle becomes wider. Spherical array antennas combine the capabilities of array antennas with the optimal geometry to achieve omni-directional coverage (Fig. 1). Spherical antennas are much more difficult to model and design than planar antennas and after early theoretical and experimental works [1-6] spherical arrays have received much less attention than other types of array antennas. Recently, there has been a growing interest in designing spherical antenna arrays and different aspects of design challenges have been analyzed [7-11].

Radiation pattern of the antenna array is defined by geometrical distribution of antennas and characteristics of antenna feeding. Achievement of the desired pattern shape depends on the geometric precision and accuracy of the feeders phase distribution. Precise distribution of the feeders phase is the topic of interest in different articles (see for example [10, 12]). Only few of the research articles deal with positional errors (e.g. [13]), but none for spherical arrays.

In the fabrication of spherical arrays positional errors are possible due to inconvenient geometry. This work gives a systematic analysis of different positional errors of the individual antenna in a spherical array and its influence on the radiation pattern.

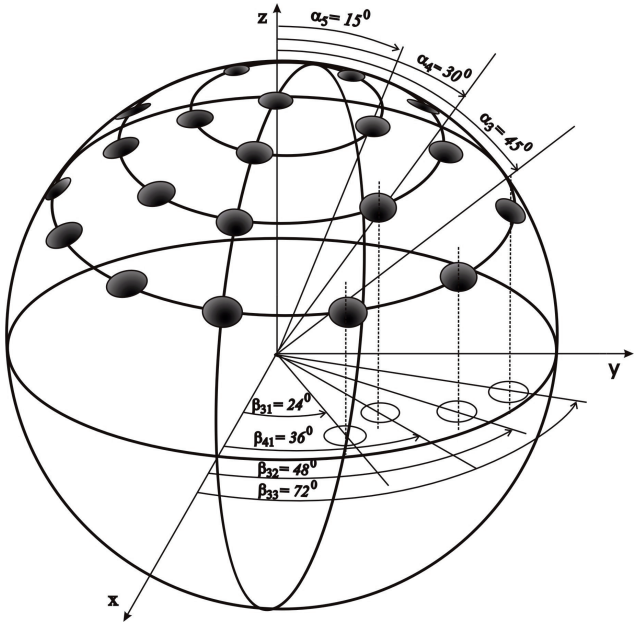


**Fig. 1.** Geometrical representation of the antenna element distribution on spherical surface [19].

## 2. Far Field Calculation of Spherical Arrays

For the purpose of a far field calculation a rigorous analysis of the spherical aperture array (Fig. 1) is performed using the spectral-domain approach. The starting point for the analysis is the electric field integral equation (EFIE) and the moment method (MoM). The spectral-domain technique transforms a three-dimensional problem into a spectrum of one-dimensional problems, which is much easier to solve [14], [15]. Since the radiating structure is spherical, the problem is defined in the spherical coordinate system and this spectrum is obtained by applying the vector-Legendre transformation to the equivalent current at waveguide aperture [16], [17]. An electrical field radiated by the current shell on the spherical surface in homogeneous media is:

$$\mathbf{E}(r,\theta,\phi)=\sum_{m=-\infty}^{\infty}\sum_{n=|m|}^{\infty}\overline{\overline{\mathbf{L}}}(n,m,\theta)\overline{\overline{\widetilde{\mathbf{G}}}}(n,m,r\,|\,r_s)\widetilde{\mathbf{C}}(r,n,m)e^{jm\phi} \quad (1)$$

where $m$ and $n$ are the variables in the spectral domain, $\overline{\overline{\widetilde{\mathbf{G}}}}(n,m,r\,|\,r_s)$ is a spectral domain dyadic Green's function for a grounded spherical surface, $\overline{\overline{\mathbf{L}}}(n,m,\theta)$ is the kernel of the vector - Legendre transformation and $\widetilde{\mathbf{C}}(r,n,m)$ is a spectral domain current placed at each antenna element (for example: in the case of a spherical waveguide-feed aperture array $\widetilde{\mathbf{C}}(r,n,m)=\widetilde{\mathbf{M}}(r,n,m)$ - equivalent magnetic current at the open of each waveguide):

$$\widetilde{\mathbf{C}}(r,n,m)=\frac{1}{2\pi S(n,m)}\cdot$$

$$\int_{-\pi}^{\pi}\int_{0}^{\pi}\overline{\overline{\mathbf{L}}}(n,m,\theta)\mathbf{C}(r,\theta,\phi)\sin\theta\, e^{-jm\phi}d\theta\, d\phi\,, \quad (2)$$

$$\mathbf{C}(r,\theta,\phi)=\sum_{m=-\infty}^{\infty}\sum_{n=|m|}^{\infty}\overline{\overline{\mathbf{L}}}(n,m,\theta)\widetilde{\mathbf{C}}(r,n,m)\,e^{jm\phi}\,. \quad (3)$$

The kernel of the integral operator is Green's function, which is different for different structures.

The appropriate spectral-domain Green's function of a multilayer spherical structure is calculated using the G1DMULT algorithm [15].

The far field radiation patterns of a spherical array are obtained as follows. If we consider for example the $\phi$-component of the electric field in the outermost region, we have only outward-traveling waves described by $a_{nm}^{i}\hat{H}_n^{(2)}(k_0 r)$. Therefore, the $\phi$-component of the electric field can be related to different $r$-coordinates as:

$$\widetilde{E}_\phi(r_1,n,m)=\widetilde{E}_\phi(r_2,n,m)\frac{r_2}{r_1}\frac{\hat{H}_n^{(2)}(k_0 r_1)}{\hat{H}_n^{(2)}(k_0 r_2)}\approx$$

$$\widetilde{E}_\phi(r_2,n,m)\frac{r_2}{r_1}\frac{j^{n+1}e^{-jk_0 r_1}}{\hat{H}_n^{(2)}(k_0 r_2)} \quad (4)$$

where $r_1$ and $r_2$ represent the $r$-component of the far field pattern [18]. The final solution is obtained by superposing the spectral solutions.

When calculating the far field of a spherical array it is convenient to introduce local coordinate systems with the origin located at the center of each antenna element. The coordinates in the local coordinate system are determined by using the following equations (see [4] and [19]):

$$\cos\theta'=\sin\alpha_n\sin\theta\cos(\phi-\beta_{nm})+\cos\alpha_n\cos\theta, \quad (5)$$

$$\cot(\phi'-\beta_{nm})=\frac{\cos\alpha_n\sin\theta\cos(\phi-\beta_{nm})-\sin\alpha_n\cos\theta}{\sin\theta\sin(\phi-\beta_{nm})} \quad (6)$$

where $\alpha_n$ and $\beta_{nm}$ are the $\theta$ and $\phi$ coordinates of each antenna element in the global coordinate system. The geometry of the problem is shown in Fig. 1 and Fig. 2.

The radiation pattern of the array is obtained as a superposition of fields excited by each antenna element (placed on a spherical surface at the point with coordinate $(\alpha_n, \beta_{nm},)$ (see [4]):

$$E_{\theta,\alpha_n,\beta_n}(\theta,\phi)=-\frac{\cos\theta\sin\alpha_n\cos(\phi-\beta_{nm})-\sin\theta\cos\alpha_n}{\sin\theta'}\cdot$$

$$E_\theta(\theta',\phi')-\frac{\sin\alpha_n\sin(\phi-\beta_{nm})}{\sin\theta'}E_\phi(\theta',\phi')\,, \quad (7)$$

$$E_{\phi,\alpha_n,\beta_n}(\theta,\phi)=\frac{\sin\alpha_n\sin(\phi-\beta_{nm})}{\sin\theta'}E_\theta(\theta',\phi')-$$

$$\frac{\cos\theta\sin\alpha_n\cos(\phi-\beta_{nm})-\sin\theta\cos\alpha_n}{\sin\theta'}E_\phi(\theta',\phi')\,. \quad (8)$$

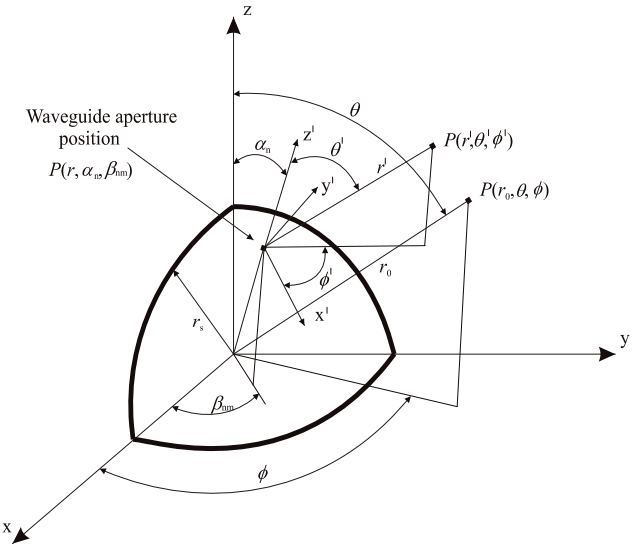


**Fig. 2.** Spherical array geometry with a global and local coordinate system used.

The complete pattern expression of the field produced by the array is given as:

$$\mathbf{E}(\theta,\phi)=\sum_{n,m}\mathbf{E}_{\alpha_n\beta_n}(\theta,\phi)\,. \quad (9)$$

In this analysis, antenna elements are excited with uniform amplitude, but they are not phased.

# 3. Spherical Array Fabrication Errors

In order to investigate spherical array fabrication errors we have developed a MoM based computer program and built a laboratory model of a spherical waveguide array.

The effect of three groups of fabrication errors on the far field radiation pattern is investigated:

a) dimension errors – errors of the spherical surface radius and functional important dimension of elementary antenna (for example: waveguide radius ($r_{serr}$, $r_{werr}$));

b) errors of elevational and azimuthal position of each antenna element ($\alpha_{2err}$, $\beta_{2err}$) (see Fig. 3 and Fig. 4);

c) errors of local angles ($\theta'_{2err}$, $\phi'_{2err}$) (Fig. 5 and Fig. 6).

## 3.1 Experimental Model Errors

The fabricated model consists of 6 waveguide elements on the spherical surface and it is chosen for experimental investigation (see antenna distribution in Fig. 1). The model was built from an aluminium sphere on which waveguides were mounted at position with: elevation angles $\alpha_1 = 0°$, $\alpha_2 = 56°$ and azimuthal angles $\beta_{11} = 0°$, $\beta_{21} = 36°$, $\beta_{22} = 108°$, $\beta_{23} = 180°$, $\beta_{24} = 252°$, $\beta_{25} = 324°$.

Antenna elements are placed at equidistant position on the surface of icosahedrons [1]. All the array elements (waveguides) are excited in the same phase and amplitude.

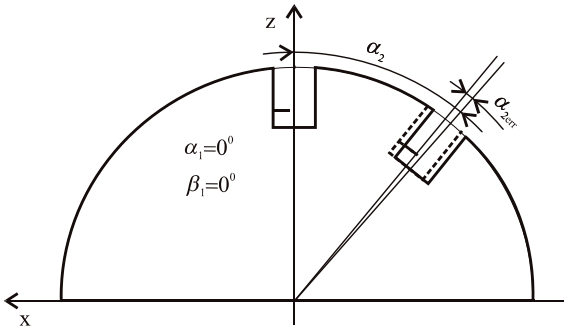


**Fig. 3.** Elevational position of the second waveguide $\alpha_2$ and elevational position error $\alpha_{2err}$.

All three groups of model errors are included in the moment method program by adding errors to their default values:

$$r_{se} = r_s + r_{serr};\ r_{we} = r_w + r_{werr}, \tag{10}$$

$$\alpha_{2e} = \alpha_2 + \alpha_{2err};\ \beta_{2e} = \beta_2 + \beta_{2err}, \tag{11}$$

$$\theta'_e = \theta' + \theta'_{2err};\ \phi'_e = \phi' + \phi'_{2err} \tag{12}$$

where $\theta'$ and $\phi'$ are coordinates in the local coordinate system (see equations (5) and (6)) [20].

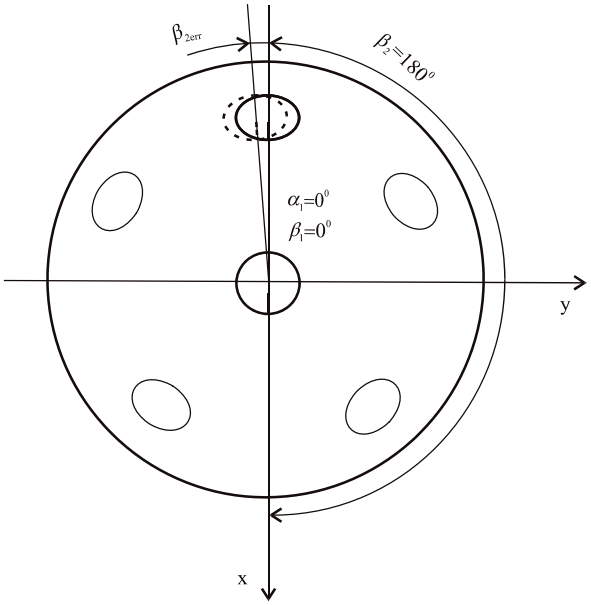


**Fig. 4.** Azimuthal position of the second waveguide $\beta_2$ and azimuthal position error $\beta_{2err}$.

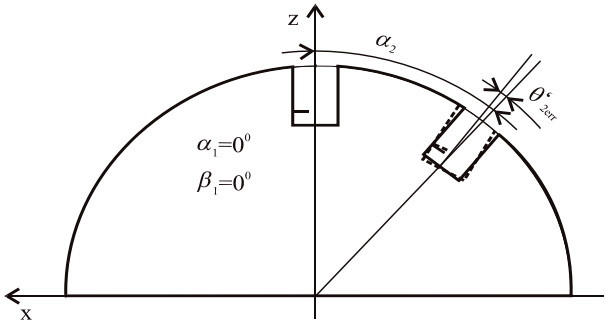


**Fig. 5.** Elevational position of the second waveguide $\alpha_2$ and local angle error $\theta'_{2err}$.

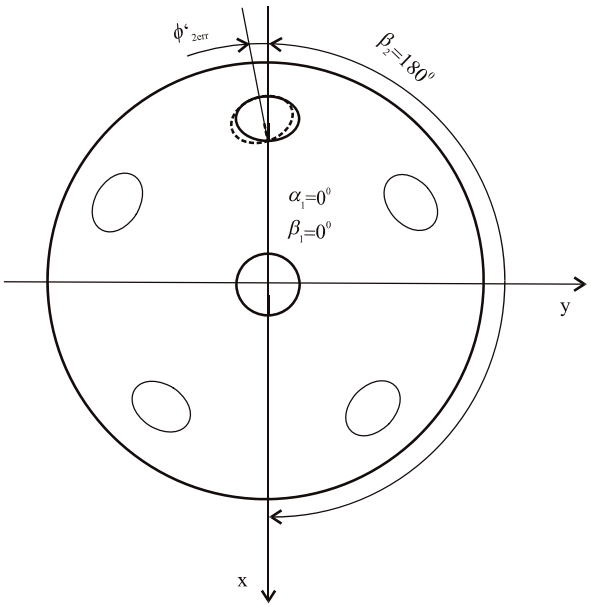


**Fig. 6.** Azimuthal position of the second waveguide $\beta_2$ and local angle error $\phi'_{2err}$.

The influence of these errors of a spherical model was rigorously analyzed for two waveguides of the spherical arrays: the first (central) with coordinates ($\alpha_1$, $\beta_1$) and the second waveguide with coordinates ($\alpha_2$, $\beta_2$). Because of that, for azimuthal position of the second waveguide we used only one index ($\beta_2 = \beta_{23}$).

We have also analyzed six waveguide-feed aperture antenna spherical array.

# 4. Numerical and Measured Results

An appropriate experimental antenna is designed with circular waveguides used as antenna elements placed on (into) the spherical structure.

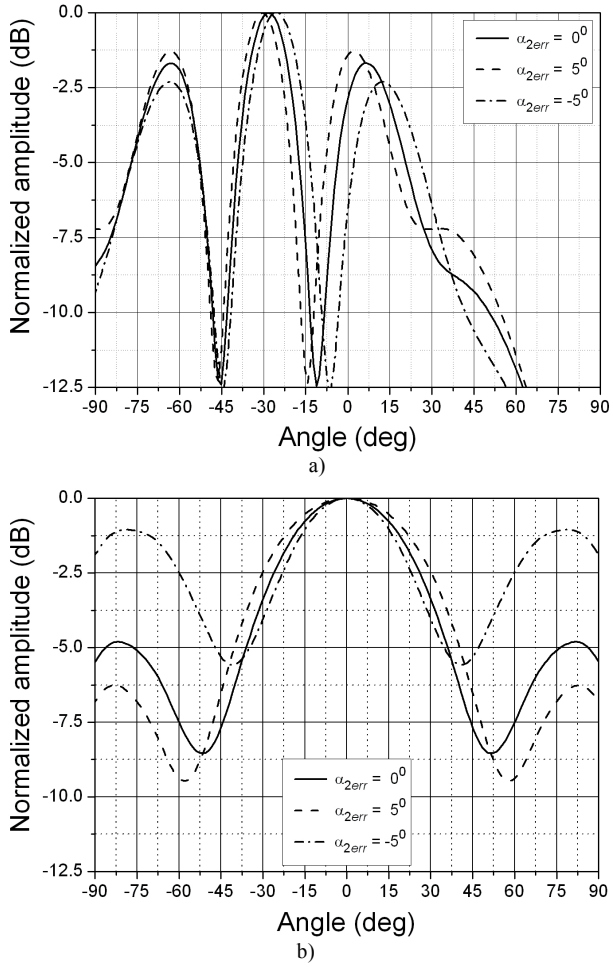


**Fig. 7.** Radiation pattern of two waveguides of the spherical array with elevational position error $\alpha_{2err}$ as a parameter: a) E-plane; b) H-plane.

Two waveguide spherical array design specifications (default values – values without errors) of the analyzed parameter are:

- first waveguide position: $\alpha_1 = 0°$, $\beta_1 = 0°$;
- second waveguide position: $\alpha_2 = 56°$, $\beta_2 = 180°$;
- radius of the spherical surface: $r_s = 30$ cm and
- waveguide radius: $r_w = 6$ cm.

In a case of spherical array of six circular waveguide fed apertures spacing of the adjacent waveguides along the circumference of the 56 degree circular ring is 1.82 $\lambda_0$, and spacing of the north pole waveguides and ring waveguides is 1.71 $\lambda_0$.

Further, normalized radiation patterns and differential radiation patterns were calculated and measured at the frequency $f$ = 1.75 GHz for E and H plane. Antenna arrays were oriented in a fixed position and both E- and H- plane patterns were recorded.

Radiation patterns produced by the experimental model were measured over the azimuthal angle ranging between -90$^0$ and 90$^0$.

When the influence of a particular parameter on the radiation pattern is calculated, other parameters have their default values.

The far field radiation patterns of the theoretical model without positional errors (solid line) and with included errors are shown in Figs 7 – 10.

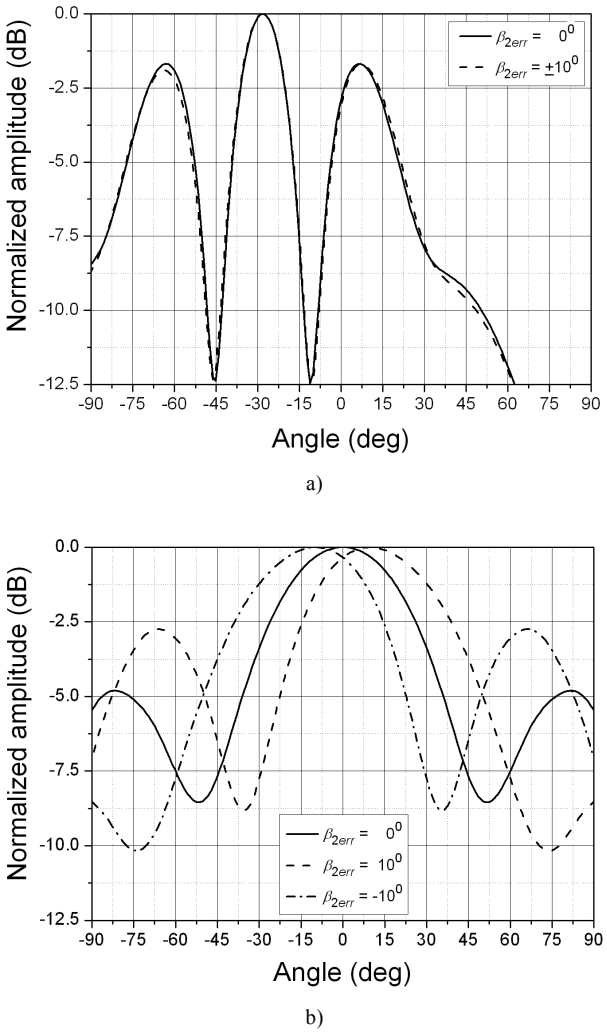


**Fig. 8.** Radiation pattern of two waveguides of the spherical array with azimuthal position error $\beta_{2err}$ as a parameter: a) E-plane; b) H-plane.

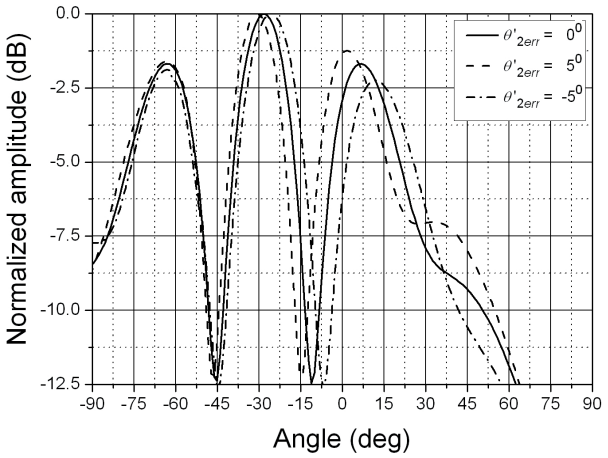


a)

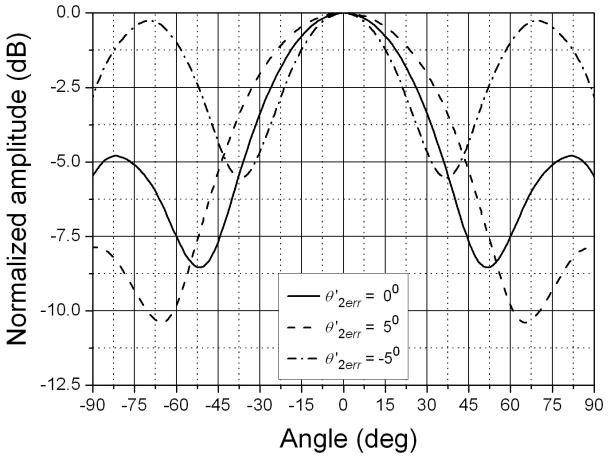


b)

**Fig. 9.** Radiation pattern of two waveguides of the spherical array with local angle error $\theta'_{2err}$ as a parameter: a) E-plane; b) H-plane.

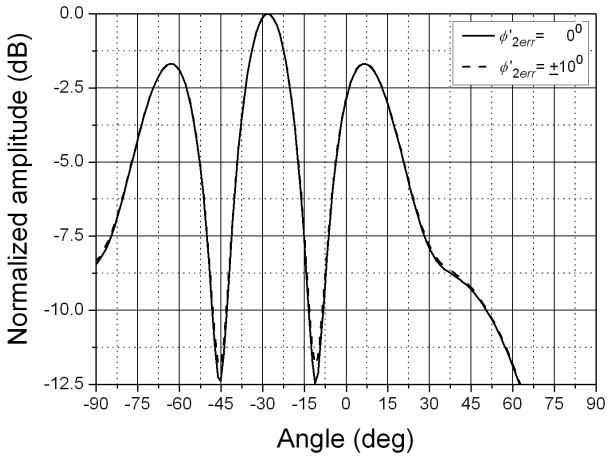


a)

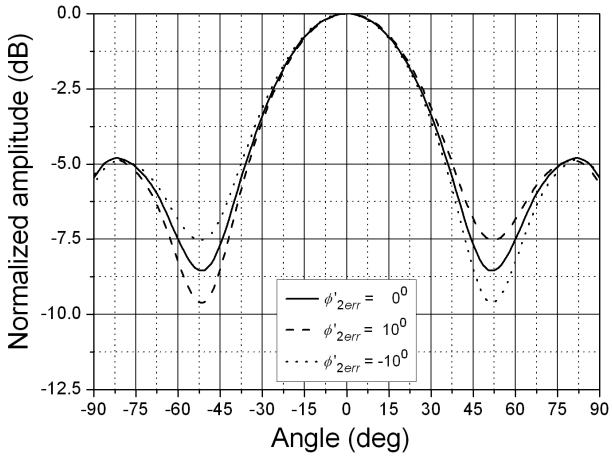


b)

**Fig. 10.** Radiation pattern of two waveguides of the spherical array with local angle error $\phi'_{2err}$ as a parameter: a) E-plane; b) H-plane.

As we expected, the main beam peak of the radiation pattern (for E-plane) is (without errors) on a half value of the second waveguide position angle:

$$\theta_{mbp\,t} = \frac{\alpha_2}{2} = 28^{\circ} \quad \text{(E-plane)} \tag{13}$$

where $\theta_{mbp\,t}$ is the angle of the main beam peak position and index $t$ means a theoretical model.

By comparing the results computed for elevation position errors $\alpha_{2err}$ (Fig. 7) and local elevation angle errors $\theta'_{2err}$ (Fig. 9) it can be concluded that this type of errors has a similar effect on the radiation pattern. For positive values of this type of errors in E-plane, the pattern is shifted in negative angle direction and the side lobe levels are also increased. For negative error values the influence is reversed. In H-plane, positive angle errors decrease and negative increase the side lobe levels (Figs 7b and 9b).

Azimuthal position errors $\beta_{2err}$ and local azimuthal angle errors $\phi'_{2err}$ have similar effects on the radiation pattern (Figs 8 and 10).

In the case of H-plane azimuthal position errors $\beta_{2err}$, the radiation pattern becomes asymmetric when azimuthal position errors become different from zero.

It is observed that the radiation pattern may not change significantly with respect to the change of dimension errors ($r_{serr}$, $r_{werr}$) except in the case of H-plane waveguide radius errors where the side lobe levels increase with negative values of waveguide radius errors and decrease with positive values (Figs. 11 and 12).

| $\beta_{nm}$ (deg) | $\alpha_{err}$ (deg) | $\theta'_{err}$ (deg) | $\beta_{err}$ (deg) | $\phi'_{err}$ (deg) |
|---|---|---|---|---|
| 36 | 0 | +2.0 | -2.5 | +9 |
| 108 | +1.0 | +3.5 | -1.0 | -13 |
| 180 | +2.0 | +5.0 | 0 | 0 |
| 252 | 0 | +6.0 | +2.0 | +13 |
| 324 | 0 | -2.0 | -1 | -8 |

**Tab 1.** Errors in the fabrication of the six waveguide antenna arrays.

Theoretical and measured free–space normalized radiation patterns of two waveguide antennas on the spherical surface are shown in Fig. 13. Included fabrication

errors are: $\alpha_{2err}$ = 2°, $\beta_{2err}$ = 0°, $\theta'_{2err}$ = 5°, $\phi'_{2err}$ = 0°, $r_{serr}$ = 0 cm and $r_{werr}$ = 0 cm. With included fabrication errors the radiation pattern shifted in negative angle direction and approached the measured pattern.

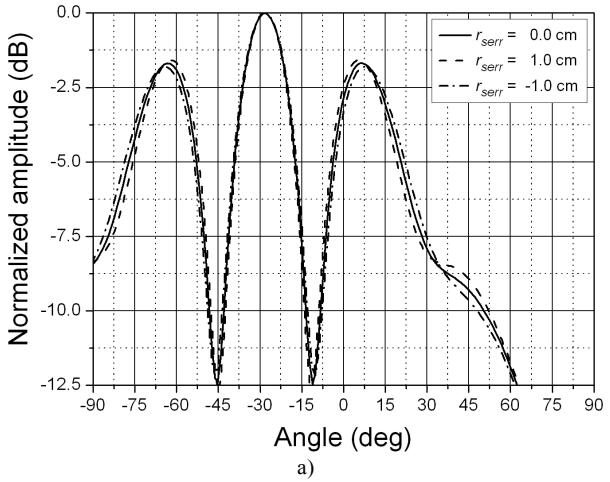


a)

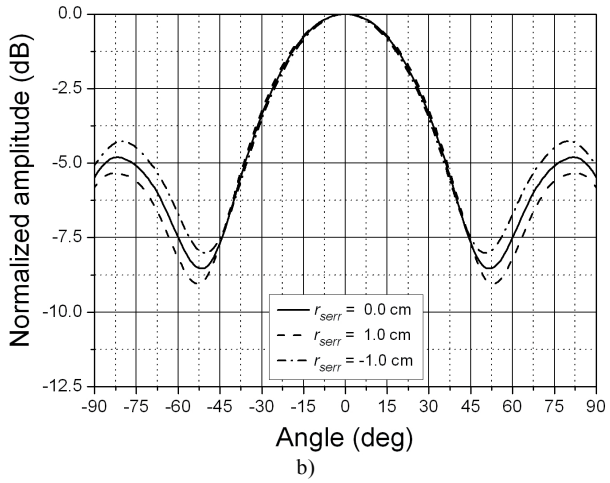


b)

**Fig. 11.** Radiation pattern of two waveguides of the spherical array with radius of the sphere $r_{serr}$ as a parameter: a) E-plane; b) H-plane.

Experimental model errors of the six waveguide spherical models that have significant influence on the radiation pattern were intentionally inserted and calculations were performed using these values of errors. The values of these errors are shown in Tab. 1.

The dimension errors $r_{serr}$, $r_{werr}$ do not have significant values.

The comparison between the measured and calculated (with and without inserted errors) far field radiation pattern of six waveguide spherical arrays is given in Fig.14.

It can be seen that with inserted measured errors it is possible to achieve a good convergence of theoretical and measured results. For a real system (antenna array) it is important to find model errors as good as possible.

This analysis was performed with an assumption that mathematical model errors and measurement errors are negligible in comparison with experimental model errors.

However, by including model errors in the theoretical model a very good agreement is achieved between the theoretical and the measured normalized radiation pattern.

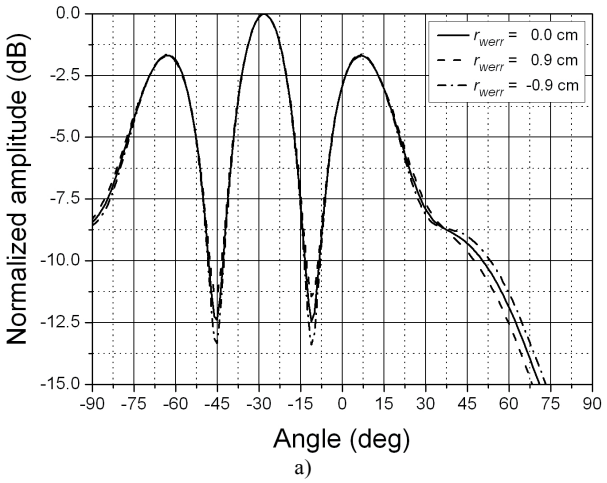


a)

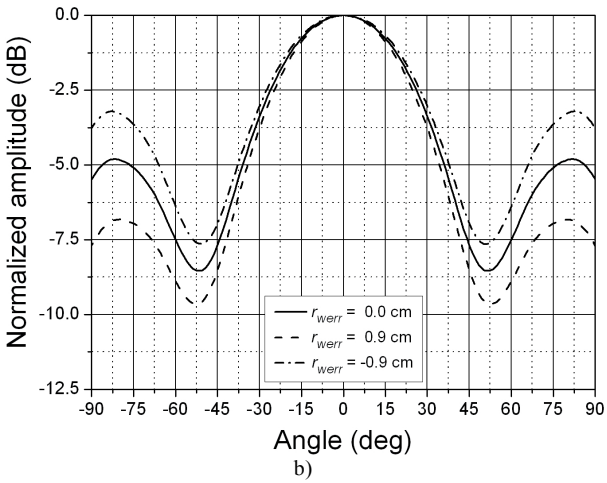


b)

**Fig. 12.** Radiation pattern of two waveguides of the spherical array with waveguide radius $r_{werr}$ as a parameter: a) E-plane; b) H-plane.

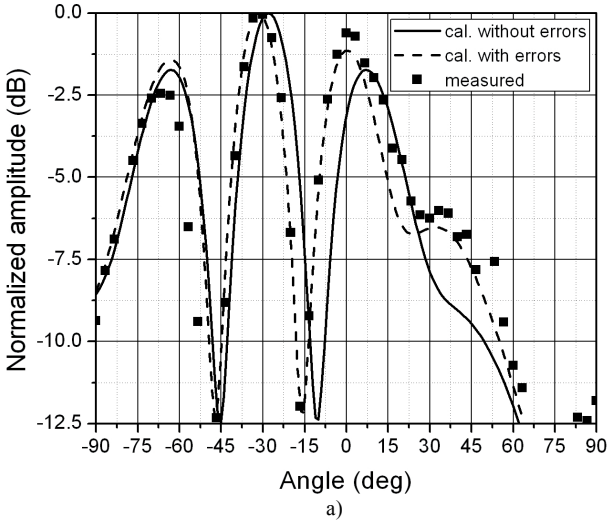


a)

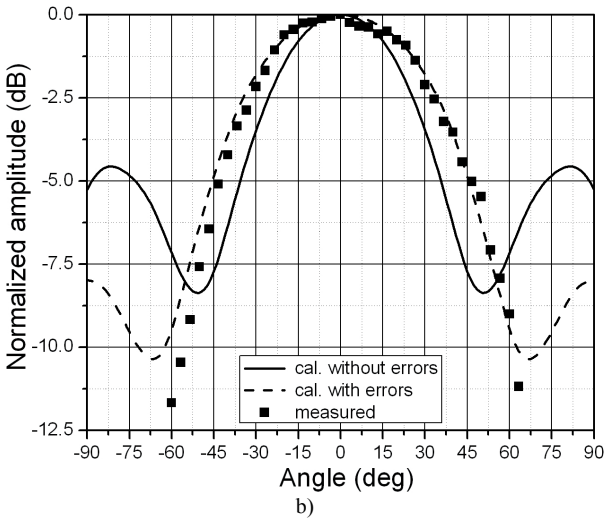


b)

**Fig. 13.** Measured and calculated radiation pattern of two waveguides of the spherical array with included fabrication error corrections: a) E-plane, b) H-plane.

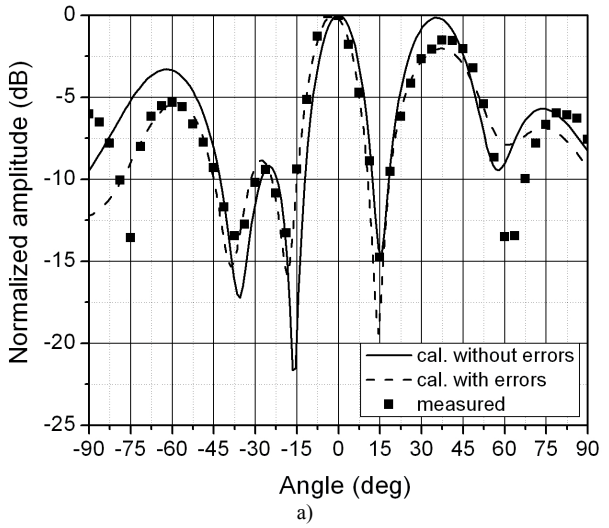


a)

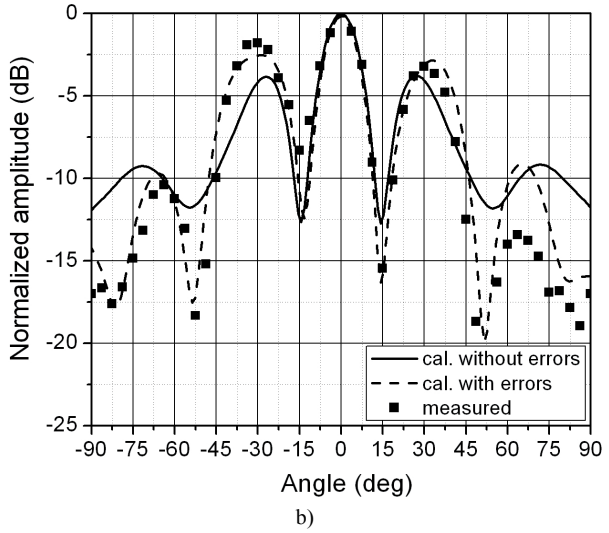


b)

**Fig. 14.** Measured and calculated radiation pattern of six waveguide spherical array with included fabrication error corrections: a) E-plane, b) H-plane.

# 5. Conclusion

This paper presents the influence of specified errors on a far field radiation pattern of the spherical antenna array. Error analysis was made with the developed moment method program that analyzes the influence of an azimuth and elevation position and local angle errors of an elementary antenna as well as model dimension errors on the radiation pattern.

We achieve a very good agreement between the theoretical and the measured radiation patterns.

The phasing (incident phase shift) of the array to obtain the orientation of the main beam in favorite direction was not performed.

Measurement was performed in a chamber with negligible electromagnetic echoe.

Other possible fabrication errors like probe length, distance probe-last waveguide wall, non–ideal shape of spherical surface, etc. are not included in this study.

# References

[1] RUTZ-PHILIPP, E. M. Spherical retrodirective array. *IEEE Trans. on Antennas and Propagation*, 1964, p. 187-194.

[2] SENGUPTA, D. L., FERRIS, J. E., LARSON, R., SMITH, T. M. Azimuth and elevation direction finder study. Radiation Lab., University of Michigan, *Ann.Arbor, Rept. 7577-1-Q, AD 479635L*, 1965., *Rept. 7577-2-Q*, 1966.

[3] SENGUPTA, D. L., FERRIS, J. E., SMITH, T. M. Experimental study of a spherical array of circularly polarized elements. *Proceedings of the IEEE*, 1968, p. 2048-2051.

[4] SENGUPTA, D. L., SMITH, T. M., LARSON, R. W. Radiation characteristics of spherical array of circularly polarized elements. *IEEE Trans. on Antennas and Propagation*, 1968, vol. 16, p. 2-7.

[5] CHAN, A. K., SIGELMANN, R. A. Experimental investigation on spherical arrays. *IEEE Trans. on Antennas and Propagation*, 1969, p. 348-349.

[6] HESSEL, A., LIU, Y.-L., SHMOYS, J. Mutual admittance between circular apertures on a large conducting sphere. *Radio Science*, 1979, vol. 14, no. 1, p.35-41.

[7] KHAMAS, S. K. Electromagnetic radiation by antennas of arbitrary shape in a layered spherical media. *IEEE Trans. on Antennas and Propagation*, 2009, vol. 57, no. 12, p. 3827-3833.

[8] STUART, H. R. Eigenmode analysis of small multielement spherical antennas. *IEEE Trans. on Antennas and Propagation*, 2008, vol. 56, no. 9, p. 2841-2851.

[9] FRANEK, O., PEDERSEN, G. F., ANDERSEN, J. B. Numerical modeling of a spherical array of monopoles using FDTD method. *IEEE Trans. on Antennas and Propagation*, 2006, vol. 54, no. 7, p. 1952-1963.

[10] GOOSSENS, R., BOGAERT, I., ROGIER, H. Phase-mode processing for spherical antenna arrays with a finite number of antenna elements and including mutual coupling. *IEEE Trans. on Antennas and Propagation*, 2009, vol. 57, no. 12, p. 3783-3790.

[11] KORETZ, A., RAFAELY, B. Dolph–Chebyshev beampattern design for spherical arrays. *IEEE Transactions on Signal Processing,* 2009, vol. 57, no. 6, p. 2417 – 2420.

[12] YAN, S.-H., CHU, T.-H. A beam-steering antenna array using injection locked coupled oscillators with self-tuning of oscillator free-running frequencies. *IEEE Trans. on Antennas and Propagation*, 2008, vol. 56, no. 9, p. 2920-2928.

[13] PETKO, J. S., WERNER, D. H. Positional tolerance analysis and error correction of micro-UAV swarm based antenna arrays. In *Antennas and Propagation Society International Symposium*, 2009. APSURSI '09. IEEE, 2009, p. 1-4.

[14] KILDAL, P.-S., SANFORD, J. Analysis of conformal antennas by using spectral domain techniques for curved structures. In *Proceedings of COST 245 - ESA workshop on active antennas*, Noordwijk, 1996, p. 17-26.

[15] SIPUS, Z., KILDAL, P.-S., LEIJON, R., JOHANSSON, M. An algorithm for calculating Green's functions for planar, circular cylindrical and spherical multilayer substrates. *Applied Computational Electromagnetics Society Journal*, 1998, vol. 13, p. 243-254.

[16] LEIJON, R. Radiation from mobile phone antennas close to the human body. *Technical Report No.270L*, Department of Microwave Technology, Chalmers University of Technology, Gothenburg, 1997.

[17] TAM, W. Y., LUK, K. M. Resonances in spherical-circular microstrip structures. *IEEE Trans. on Microwave Theory Tech*., 1991, vol. MTT-39, p. 700-704.

[18] SIPUS, Z., RUPCIC, S., LANNE, M., JOSEFSSON, L. Analysis of circular and spherical array of waveguide elements covered with radome. In *Proceedings of IEEE International Symposium on Antennas and Propagation.* Boston (USA), 2001, p. 350-353.

[19] RUPCIC, S. Circular waveguide antenna arrays on spherical structures. *PhD dissertation,* University of Zagreb, Faculty of Electrical Engineering and Computing, Zagreb, 2009.

[20] RUPCIC, S., MANDRIC, V. Model errors of a spherical aperture antennas array. In *SIP 2008*. Osijek (Croatia), 2008, p. 21 - 26.

## About Authors ...

**Slavko RUPCIC** received his B.Sc. degree in electrical engineering from University of Split, Faculty of Electrical Engineering, Mechanical Engineering and Naval Architecture, in 1989. He received his M.Sc. and Ph.D. degree in electrical engineering from University of Zagreb, Faculty of Electrical Engineering and Computing, in 1994 and 2009, respectively. Since 1990 he has worked at the Faculty of Electrical Engineering, University of Osijek in the Department of Communications - Laboratory for HF measurements. In recent years, he has been involved in different research activities including measurement, modeling and simulation of different radiating structures on conformal surfaces. His research interests include antenna analysis, numerical computation of radiating structures and radio communications systems. He is a member of IEEE, Antenna and Propagation Society.

**Vanja MANDRIC** received her B.Sc. degree in electrical engineering from J. J. Strossmayer University of Osijek in 2005. Since 2005 she has been an assistant at the Faculty of Electrical Engineering, University of Osijek in the Department of Communications - Laboratory for HF measurements. Vanja Mandric's research interests include areas of antenna analysis, numerical computation of radiating structures and radio communications systems.

**Snjezana RIMAC-DRLJE** received her B.Sc., M.Sc. and Ph.D. degree in electrical engineering from Zagreb, Faculty of Electrical Engineering and Computing, in 1987, 1994 and 2000, respectively. Since 1987 she has worked at the Faculty of Electrical Engineering, University of Osijek, where she is currently Associate Professor in the Department of Communications, and Head of the Laboratory for HF measurements. From 2001 to 2003 she was Vice-Dean for Education and from 2003 to 2005 she was Vice-Dean for Science. Dr. Rimac-Drlje's research interests include image/video compression, wavelet transform, image/video processing, video quality evaluation and wireless communication systems. She is a member of IEEE, Communication Society and SPIE.